

Reconstruction of subsurface layers of sediments in the estuaries Parak and Shoor by using ground-penetrating radar

Mohyeddin AhrariRoudi

Department of Oceanography, Faculty of Marine Science, Chabahar Maritime University, Chabahar, Iran

Email: m.ahrari@cmu.ac.ir

Abstract

The study area on the North West Coast of Oman Sea in Shoor and Parak estuaries is located within Near the Chabahar. Preparation outcrops GPR to produce and record all events take place at shallow depths below surface. The GPR and seismic profiles are in order to prepare and investigate the effects of subsurface. Identification of shallow subsurface structures and thickness of the different is due to the contrast in electrical properties such as electrical conductivity. This is important objective of the study research that is done by GPR methods. In this study, the GPR profiles were taken with instrument of GPR-Mala Geoscience-3 Step charger. In order to calibration the seismic data with characteristics facies obtained by using handy coring instrument (Euger) was prepared involves two cores to lengths of 4.35 and 5 m. The data from these two methods are compared and was obtained the necessary conclusion. The study showed that the cores are composed of two sedimentary facies. The first facies set (Muddy facies) with brown color that the sedimentary environment is supratidal and the second facies set (Sandy facies) with gray color that specificities are related to depositional environment intertidal. Profiles of the Shoor estuary show up four different facies that they are consistent with the core sedimentary facies in the environment are supratidal that thickness of Subsurface layers increases from northeast toward the South West. Profile of the Parak estuary show up two different facies that they are consistent with the core sedimentary facies in the environment are supratidal that thickness of Subsurface layers does not changed from northeast toward the South West. Since, the profile GPR Numbers the 73 and 74 was nearer to the sea and influence the saltwater sea on GPR data. Thus, in Parak estuary and the effect of sea water on depth Penetration is more and detection of subsurface structures is weaker that has leading to the identification two layers of subsurface. In Shoor estuary (The profile GPR Numbers the 71 and 72), high distance from the sea and the effect of sea water on depth Penetration is less and detection of subsurface structures is stronger that has leading to the identification four layers of subsurface. On the other hand comparison of sediment cores and GPR profiles with curve changes in global sea levels show that during two-Interval time (respectively 2100 to 2800 & 4900 to 5800 years ago) sedimentation rates was higher than average (0.1 mm per year). Finally, using GPR profile and cores, sea level changes in coastal environments can be revealed. These changes indicate that the two sedimentary cycles includes of a rise and fall sea level locally in the North West estuaries of Oman Sea in connection with the tectonic situation in the region.

Keywords: Shoor, Parak, Electrical Conductivity, GPR Profiles, Chabahar, Estuary.

1. Introduction

Ground-penetrating radar (GPR) is a geophysical method that uses radar pulses to image the subsurface. This nondestructive method uses electromagnetic radiation in the microwave band (UHF/VHF frequencies) of the radio spectrum, and detects the reflected signals from subsurface structures. GPR can have applications in a variety of media, including rock, soil, ice, fresh water, pavements and structures. In the right conditions, practitioners can use GPR to detect subsurface objects, changes in material properties, and voids and cracks (Daniels DJ, 2004). GPR uses high-frequency (usually polarized) radio waves, usually in the range 10 MHz to 1 GHz. A GPR transmitter emits electromagnetic energy into the ground. When the energy encounters a buried object or a boundary between materials having different dielectric constants, it may be reflected or refracted or scattered back to the surface. A receiving antenna can then record the variations in the return signal. The principles involved are similar to seismology, except that electromagnetic energy is used instead of acoustic energy, and energy may be reflected at boundaries where subsurface electrical properties change rather than subsurface mechanical properties as is the case with seismic energy.

The electrical conductivity of the ground, the transmitted center frequency, and the radiated power all may limit the effective depth range of GPR investigation. Increases in electrical conductivity attenuate the introduced electromagnetic wave, and thus the penetration depth decreases. Because of frequency-dependent attenuation mechanisms, higher frequencies do not penetrate as far as lower frequencies. However, higher frequencies may provide improved resolution. Thus operating frequency is always a trade-off between resolution and penetration. Optimal depth of subsurface penetration is achieved in ice where the depth of penetration can achieve several thousand meters (to bedrock in Greenland) at low GPR frequencies. Dry sandy soils or massive dry materials such as granite, limestone, and concrete

tend to be resistive rather than conductive, and the depth of penetration could be up to 15-metre (49 ft). In moist and/or clay-laden soils and materials with high electrical conductivity, penetration may be as little as a few centimeters. GPR is used to map geologic conditions that include depth to bedrock, depth to the water table, depth and thickness of soil and sediment strata on land and under fresh water bodies, and the location of subsurface cavities and fractures in bedrock. Ground-penetrating radar antennas are generally in contact with the ground for the strongest signal strength; however, GPR air-launched antennas can be used above the ground.

GPR has many applications in a number of fields. In the Earth sciences it is used to study bedrock, soils, groundwater, and ice. It is of some utility in prospecting for gold nuggets and for diamonds in alluvial gravel beds, by finding natural traps in buried stream beds that have the potential for accumulating heavier particles (Wilson et al. 2006). Engineering applications include nondestructive testing (NDT) of structures and pavements, locating buried structures and utility lines, and studying soils and bedrock. In environmental remediation, GPR is used to define landfills, contaminant plumes, and other remediation sites, while in archaeology it is used for mapping archaeological features and cemeteries. GPR is used in law enforcement for locating clandestine graves and buried evidence. Military uses include detection of mines, unexploded ordnance, and tunnels. Borehole radars utilizing GPR are used to map the structures from a borehole in underground mining applications. Modern directional borehole radar systems are able to produce three-dimensional images from measurements in a single borehole (Hofinghoff, 2013).

One of the other main applications for ground-penetrating radars is for locating underground utilities. Standard electromagnetic induction utility locating tools require utilities to be conductive. These tools are ineffective for locating plastic conduits or concrete storm and sanitary sewers. Since GPR detects

variations in dielectric properties in the subsurface, it can be highly effective for locating non-conductive utilities (Zhuravlev et al. 2013). GPR is often used on the Channel 4 television programme Time Team which uses the technology to determine a suitable area for examination by means of excavations. In 1992 GPR was used to recover £150,000 in cash that kidnapper Michael Sams received as a ransom for an estate agent he had kidnapped after Sams buried the money in a field.

2. Geological and Geographical situation of the study area

Southeastern Iran or Makran zone is located to the south of Jazmurian depression. Its western boundary is Minab fault; to the south, it is restricted by the Gulf of Oman, and to the east, it extends into Pakistan. The northern part is characterized by dominance of east-west trending faults, Bashagard fault being the most important one. Along these faults lies large section of ophiolite series. The oldest rocks in this zone are the ophiolites of Late Cretaceous-Paleocene overlain by a thick sequence (about 5,000 m) of sandstone, shale, and marl. The whole sequence is deformed prior to Early Miocene. Thick sequence of Neogene rock units, in excess of 5,000 m, covers the older series (Geological Survey of Iran, 2015).

The study area is located in the south-east of Iran, north-west of the Indian Ocean, and north-east of the Oman Sea at between latitudes $25^{\circ}23'28''\text{N}$ & $25^{\circ}27'15''\text{N}$ and longitudes $60^{\circ}33'15''\text{E}$ & $60^{\circ}38'28''$ (Fig. 1). The Chabahar is in southeastern Iran. It is the only Iranian port with direct access to the ocean. The port was partially built by India in the 1990s to provide access to Afghanistan and Central Asia, bypassing Pakistan.

Makran subduction zone contains one of the largest accretionary wedges on the globe, formed by the convergence between the Eurasian and the Arabian Plates. The study area is located on the Makran coast. This area is a part of coastal Makran zone (one of the geological zones of Iran) that had undergone sea

level changes along the Late Quaternary. Makran and Zabol-Baluch in SE Iran are post-Cretaceous flysch - molasse belts which join together in SE Iran and continue to the Pakistan Baluchistan Range. The flysch sediments were deposited on the Upper Cretaceous ophiolites. The Makran Subduction Zone characterizes by the subduction of the oceanic part of the Arabian plate beneath the Eurasian plate. Makran Subduction Zone is unique region in the world due to its geological and seismological characteristics. High sediment input of 7 km, shallow angle of dip and rate of subduction are interesting and distinctive features of this zone. Oceanic lithosphere in the Arabian plate is moving north and is subducted under Lut plate and Afghan-Helmand block. The rates of both Arabic and Makran coast in the measurements geodetic is measured between Muscat and Oman 1.9 cm in years, While the current rate of shrinkage in the Makran coast and Chabahar area is measured about 8 mm in years (Vernant et al. 2004; Dolati, 2010).

3. Operations, Material and Methods

The operation of GPR was performed in the northern coast of Oman Sea in estuaries Shoor and Parak (Fig. 1). The use of GPR has been prepared to the seismic profiles and all the side effects of both natural and artificial surface. In two regions of coastal or the estuaries Shoor and Parak, using the model GPR Mala (Fig. 2) in the direction perpendicular to the sea shore of the basin upstream four profiles were conducted and survey operations (Profiles 71, 72, 73 and 74 in Fig. 1). Profiles of 71 assorted in estuary Parak began from geographical coordinates $\text{N } 25^{\circ} 26' 34''$ & $\text{E } 60^{\circ} 33' 59''$ and with 920 meters of navigation was ended the operation of GPR in coastal sand dunes on the geographical location of $\text{N } 25^{\circ} 26' 20''$ & $\text{E } 60^{\circ} 33' 22''$. Profiles of 72 in estuary Parak began from appropriate geographical coordinates $\text{N } 25^{\circ} 26' 22''$ & $\text{E } 60^{\circ} 33' 20''$ and Profiles parallel to the first 144 meters and was ended the area at the point $\text{N } 25^{\circ} 26' 17''$ & $\text{E } 60^{\circ} 33' 19''$. Profiles of 73 assorted in estuary Shoor began from geographical coordinates

N 25° 25' 38" & E 60° 38' 26" and with the 300 m survey in the direction perpendicular and crossed of the channel was ended in location N 25° 25' 35" & E 60° 38' 15". The operation continued with enthusiasm worthy of 74 profiles. The profile at a point with geographical coordinates N 25° 25' 33" & E 60° 38' 11" was ended with a scroll 630 meters and parallel to the profiles of the point N 25° 25' 24" & E 60° 37' 47". Finally the total GPR harvest operation was 1,994 meters. Required to explain, the high level of groundwater in these regions (about 3-2 m below ground level). Areas to be selected in the places that are not severe topography GPR data obtained so far have not been affected by errors caused by this factor. GPR data of four profiles in selected, after harvesting, were used processing and interpretation. In order to calibrate the seismic data obtained, two cores were prepared with lengths 35.4m and 5m sediment core L with geographic location N 25° 26' 21" & E 60° 33' 51" in parak estuary and sediment cores U and geographic location N 25° 25' 34" & E 60° 38' 19" in Shoor estuary have been produced (Fig. 1).

Methods the study included library studies and study check prior work, Field studies, laboratory studies that data have been combined. In the first part of the study, the location profiles have been recorded with GPS models Garmin-Olathe, Ks, USA. Two sediment cores was performed with the length 5m (L) in the estuary Park and with the length 35.4 m (U) in Shoor estuary by the machine manually (Euger) (Fig.

2). In the study of sediment cores, the core were described by Visual Studies in desert and others characteristics such as shape, color, sedimentary structures. In order to the breakdown of sedimentary facies, selection of sample is done and they were prepared to sedimentology laboratories in Geological Survey of Iran. 65 samples aggregated. At this stage, about 200 g of sediment was and 24 hours in distilled water was Attached to are separated from each other, The clay is used to prevent connection Shell fragmentation , The samples were exposed to ultrasound for 15 minutes in the mixer, Then sieve the sample in the Shaker style Analysette 3 Fritsch German companies were And 30 minutes to wet the seeds of different sizes were separated After drying, were weighed (Tucker, 1988), Particles of 63 microns and finer grain size by laser (Laser Particle Sizes) companies in Germany Fritsch Geological were analyzed. The types of deposits based on triangular diagrams folk (1974) has been made. In order to the processing data of sediment cores, have been used software Sediment Size, Notepad, WordPad, Photoshop CS and Excel 2007 for custom charts, tables and calculations. In the second part of the study, the profile of the GPR, Relevant data in digital memory storage device was Reflex 2D-Queeck software to help with a specific format were transferred to a personal computer. The data output was done on display by the Transform of software. Then the subsurface layers were identified. With compared results from sediment core and GPR

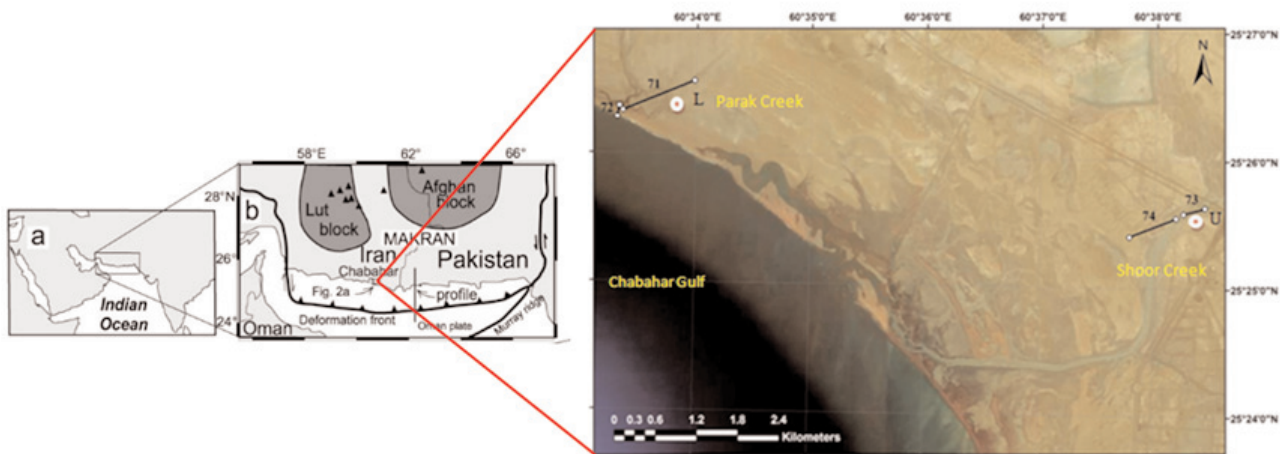


Figure. 1. Satellite photos of the area, profiles of GPR (Black line) and the sedimentary cores drilled (Red circle)

data, conclusions were. Due to the high frequencies used in this study (250 MHz) Electrical conductivity and relatively high tidal environment surface of clay layers in the study area, GPR penetration depth and the waves were very limited 6.3 m is not exceeded. Harvest operations were done a total of 1994 meters (Contains 2 profiles (1064m) in Parak estuaries and 2 profiles (930m) in Shoor estuaries).

4. Description of sediment cores and their correlated with the GPR profiles

Sediment core U: Length of the core is 4.35m that was prepared in shoor estuary (Fig. 3) and five sedimentary facies from surface to deep consist of:

Facies 1: Continues from surface to depth of 30cm and include slightly gravely sandy mud and color is brown. This facies that with shell fragment, mud crack and evaporative minerals in the Earth's surface is related to the environment Supratidal.

Facies 2: This facies of the depth of 30cm to 55cm and a depth of 4.25m to 4.35m is and gravely mud is greenish cream-colored. This facies containing marine fossils are associated with skeletal debris is related to Intertidal Environment.

Facies 3: This facies, which extends from a depth of 55cm to 70cm are cream-colored gravely sandy mud. The facies of skeletal debris and red horizons and environmental conditions Supratidal shows.

Facies 4: from 70cm depth of this facies to a depth of 4m indicates that the environment is Intertidal. The slightly gravely sandy mud sediment facies is with a little green with shell debris abundant. Reduce the amount of gravel that the components of skeletal fossils are marine, signs of rising sea levels and the environmental conditions are Intertidal.

Facies 5: in this facies from depth of 4m to a depth of 4.35m appears and deposits of mud with greenish gray colors and the environment is Intertidal.

The combined results obtained from GPR data and sedimentary cores, the GPR profiles and their compliance in estuary Shoor, it was related that the change of sedimentary facies and depositional envi-

ronment is with changes in particle size. In the GPR profiles of 73 and 74, subsurface layer 1 of with sedimentary units 1 and 2 sediment core, subsurface layer 2 with sedimentary units 3 and subsurface layers 3 and 4 are consistent with sedimentary unit 4 (Fig. 3). Since the waves with particles of sand and gravel abrasion damage to the beach from erosion of coastal outcrops of the above areas, can be attributed (Caldas et al. 2006; Sorrel et al. 2010), Therefore It seems Increased thickness of the layers identified shallow (subsurface layer 1) in the catchment area downstream in GPR profiles due to particles of sand and gravel is the wind the surface and near to shore that the longitudinal and transverse spread of relatively abundant. Therefore, this facies which gradually turn related to the environment Supratidal, intertidal, Supratidal and is intertidal and are the two sedimentary cycles include a Raise and lower the water levels locally in the northern Oman Sea.

Sediment core L: Length of the core L, 5 meters that was prepared in Parak estuary (Fig. 4) and four sedimentary facies from surface to deep consist of:

Facies 1: From the surface to a depth of 90cm of muddy sediments is very sticky and greenish cream color reagent containing evaporating deposit is Supratidal environment.

Facies 2: This facies is expanding from 90cm to the depth of 100cm. This facies consists of sandy mud sediments grayish cream color and abundant skeletal debris represents an increase in sea level and is intertidal environment.

Facies 3: From 1 meter to 1.2m of the depth and from 85.3m to 85.4m of a depth of sediment facies with muddy sand with small gravel is spread. The sedimentary facies is skeletal debris containing, grayish green colors and lamination thin. Histological features of this facies and field evidence indicate sea levels and environmental conditions is Supratidal.

Facies 4: The facies from 1.2m to 85.3m of depth and a depth of 85.4m to 5 m is expanding. The sedimentary deposits of this facies are slightly gravely sandy mud with a little green to greenish-gray, skeletal

debris and organic material. Increase the amount of mud and marine fossils, evidence of rising sea levels and environmental conditions is intertidal.

The combined results obtained from GPR data and sedimentary cores and their compliance with the GPR profile in Shoor estuary it was related that Changes in sedimentary facies and depositional environment is associated with changes in particle size. In the GPR profiles of 71 and 72, subsurface layer 1 from surface to a depth of 90 cm with facies 1 Supratidal environment and from 90 cm to 1 meter intertidal environment is consistent with facies 2. Also the subsurface layer 2 in these profiles with sedimentary units 3 are correlated environmental Supratidal (Fig.4). Therefore, this facies which gradually turn related to the environment Supratidal, intertidal, Supratidal and is intertidal and the two sedimentary cycles include a raise and fall the water levels locally in the northern Oman Sea are. On the other hand comparison of sediment cores and GPR profiles with curve changes in global sea levels show that during two-Interval from time 2100 to 2800 years ago and so from time 4900 to 5800 years ago, increased sedimentation and sedimentation rates higher than average (0.1mm per year) respectively (Fig.5).

Results of the adaptation of seismic data and sedimentary facies indicate that Changing the particle size, type and depositional environment is related to

sediments particle size in the subsurface layers.

5. Identify subsurface layers and interpretation of GPR profiles

5.1. Data processing performed on these four profiles is

Profile No.71: In this profile, there are two layers subsurface (Fig.6). Thickness of the first subsurface layer 1 about 4.1 m and thickness in the subsurface layer 2 is about 78 cm and from the top of point start move towards the sea, the layers thickness increased. The subsurface layer 1 in the profile 71 and 72 from the surface to a depth of 90 cm with facie 1 in Supratidal environment and from depth of 90 cm to one meter of depth is identical with facies 2 intertidal environment. So, the subsurface layer 2 in the GPR profiles with the sedimentary units 3 are related to environmental Supratidal. Increasing thickness of layers is due to expansion of the surface sediments of sand dunes in coastal area. Colored lines are indicated contacts between the layers red and blue areas. Depth of effect the penetration wave is not higher of 2.5m in these profiles.

Profile No.72: In this profile, there are two layers subsurface (Fig.7) and thickness of the first subsurface layer 1 about 4.1 m and thickness in the subsurface layer 2 is about 78 cm and from the top of point start move towards the sea, the layer 1 thickness increased, and an increase in the subsurface layer 2



Figure 2. View of the GPR device model Mala Geoscience-3 Step charger (right) and Core-consuming manual Euger (left).

initially increases and then decreases. In this core, a subsurface layer of the profile No.71 and No.72 of the surface to a depth of 90cm with a depth of 90cm of facies 1 and supratidal environment to a depth of one meter is consistent with facies 2 intertidal environments. So, the subsurface layer 2 in the GPR profiles with the sedimentary units 3 are related to environmental supratidal. Increasing the thickness of layers due to sand dunes and wind deposits have been developed in the downstream. Colored lines between the layers and layers of red and blue areas show consideration. Depth of effect the penetration wave in these profiles of 2.6m is not higher.

Profile No.73: In this profile, there are four layers subsurface (Fig.8). The thickness of subsurface layer 1 about 1.4 m, thickness of subsurface layer 2 about 70cm, thickness of subsurface layer 3 about 40cm and thickness of subsurface layer 4 about has about 84 cm. Also, in the GPR profiles, subsurface layer 1 with layers 1 and 2 sediment cores, subsurface layer 2 with layer 3 sediment cores and subsurface layers 3 and 4 are consistent with layer 4 in sediment cores. in the withdrawals from the beginning towards the coastline, the thickness subsurface layer 1 is almost

uniform, the thickness subsurface layer 2, first increases and then decreases, the thickness subsurface layer 3, first decreases and then increases again decreases and thickness subsurface layer 4, first increases and then decreases again increases. Thickness changes due to local sea level change that have been deposited tidal sediments. Colored lines between the layers and layers of red and blue areas show consideration. Depth of effect the penetration wave in these profiles of 3.6m is not higher.

Profile No.74: In this profile, there are four layers subsurface (Fig 9). The thickness of subsurface layer1 about 70cm, thickness of subsurface layer 2 about 1.2m, thickness of subsurface layer 3 about 70cm and thickness of subsurface layer 4 about 80cm. Also, in the GPR profiles, subsurface layer 1 with layers 1 and 2 sediment cores, subsurface layer 2 with layer 3 sediment cores and subsurface layers 3 and 4 are consistent with layer 4 in sediment cores. Therefore, in the withdrawals from the beginning to the end, the thickness of first layer up to 530m area approximately uniform, and then sharply decreases. This reduction in thickness due to relative sea level change and water underground. From The first line

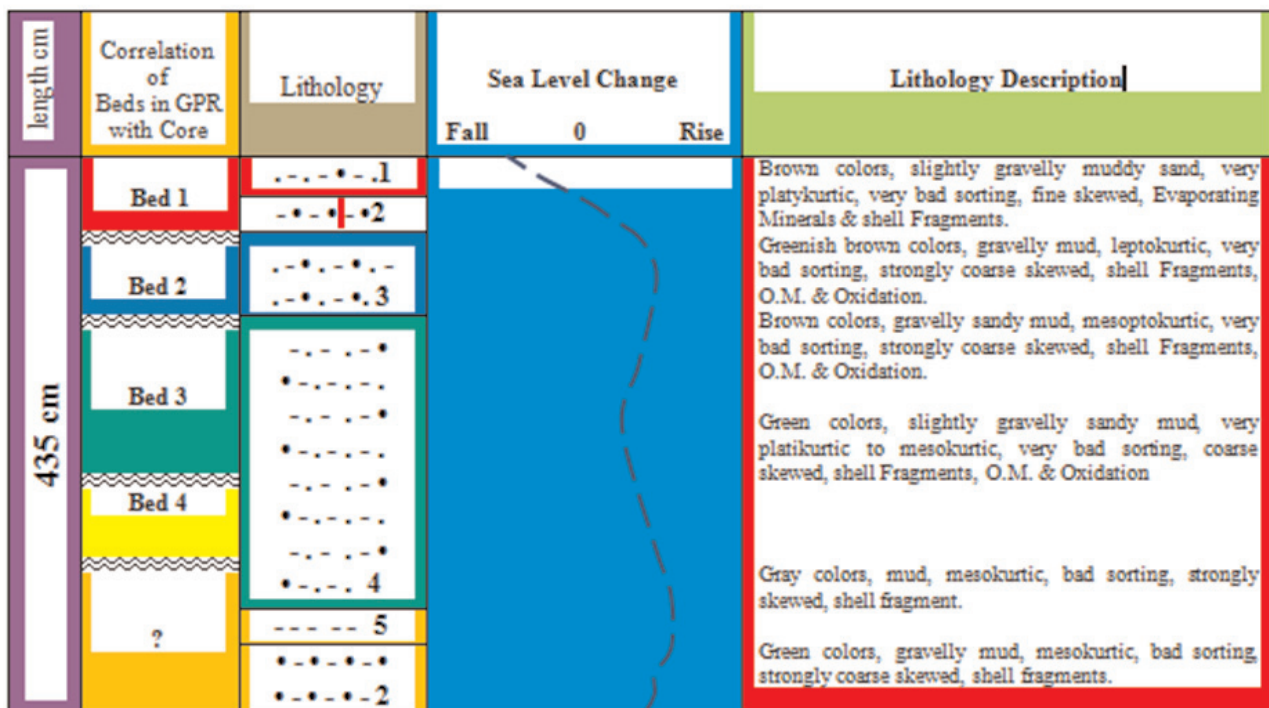


Figure 3. Correlation of layers subsurface in GPR with sediment Core, column facies, relative sea level changes and describes the sediment core U, shore estuary, scale: 1:100

toward the sea the thickness subsurface layer 2 increases. At first the thickness subsurface layer 3 decreases and then increases and the thickness subsurface layer 4 increases and so then decreases again increases. Thickness changes due to local sea level change that have been deposited tidal sediments. Colored lines between the layers and layers of red and blue areas show consideration. Depth of effect the penetration wave in these profiles of 3.5m is not higher.

Since, the profile GPR No.73 and No.74 was nearer to the sea and influence the saltwater sea on GPR data. Thus, detection of subsurface structures is less effective and two layers of subsurface has been identified in the Parak estuary, and so in Shoor estuary (the profile GPR No.71 and No.72), high distance from the sea and influence the saltwater sea is less and detection of subsurface structures is stronger that has leading to the identification of four layers of subsurface. As can be seen, Differences in sediment type, grain size and amount of clay in the subsurface structures, creates contrast in electrical properties, including differences in the size of the electric permittivity

of free space are the main reason for classification theirs in different layers.

Sediments set of Related to the intermediate environment are in the study area and the oldest unit is deposits of the supratidal. These sediments (A set of fine sediment includes silt and clay particles) that were sediments between intertidal due to going back to sea (falling sea level) are located above the supratidal zone. Intertidal deposits in Oman coastal composed of mud sediment, silt and sand with a tissue adhesive and Includes asymmetrical current ripple, bioturbation and symmetrical current ripple and brands are the wave of especially in coastal estuaries and the coastal strip are a lot of expansion.

6. Results

1-Sedimentary facies of the study area be related to the intertidal zone (younger unit) and supratidal zone (older unit).

2-Sedimentary facies include slightly gravely sandy mud, gravely mud, gravely sandy mud, muddy sand and sandy mud.

3-The combined results obtained from GPR data and

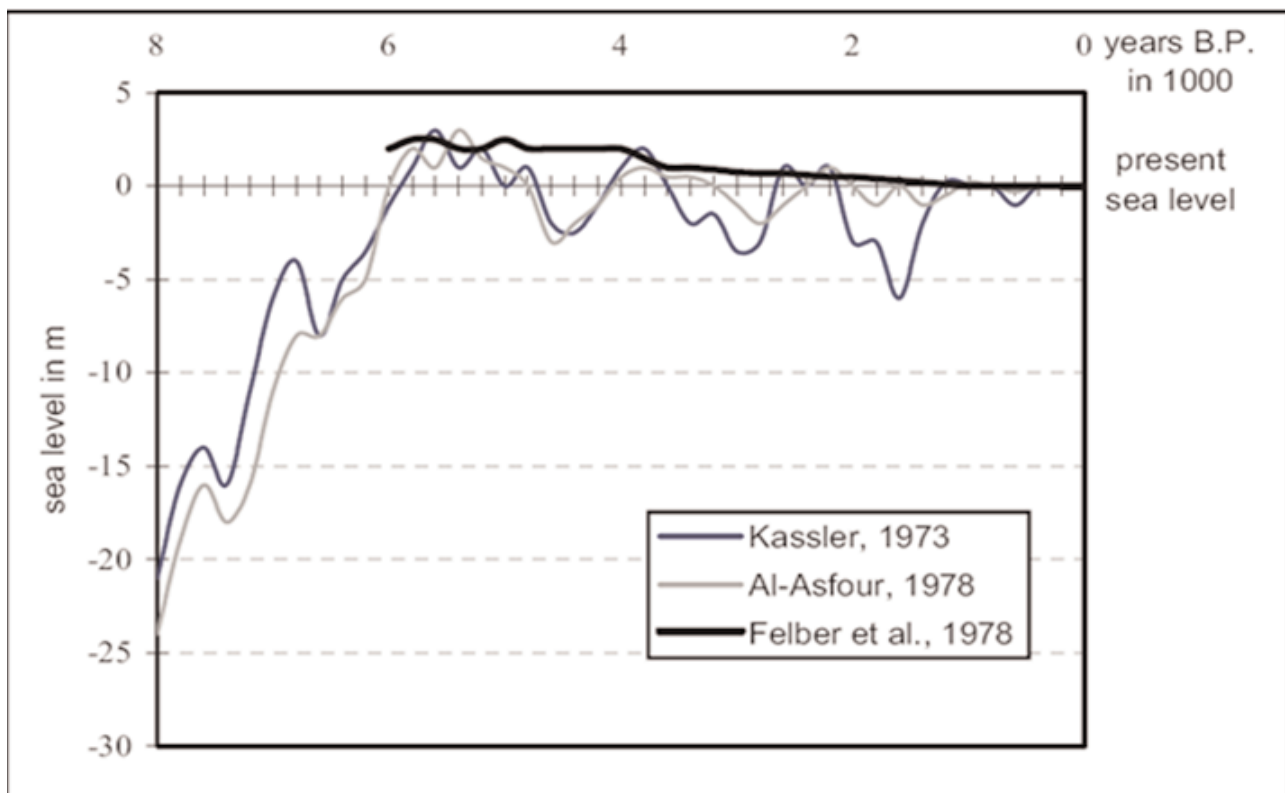


Figure 4. Sea level curve in global scale (From Uchupi et al. 1996)

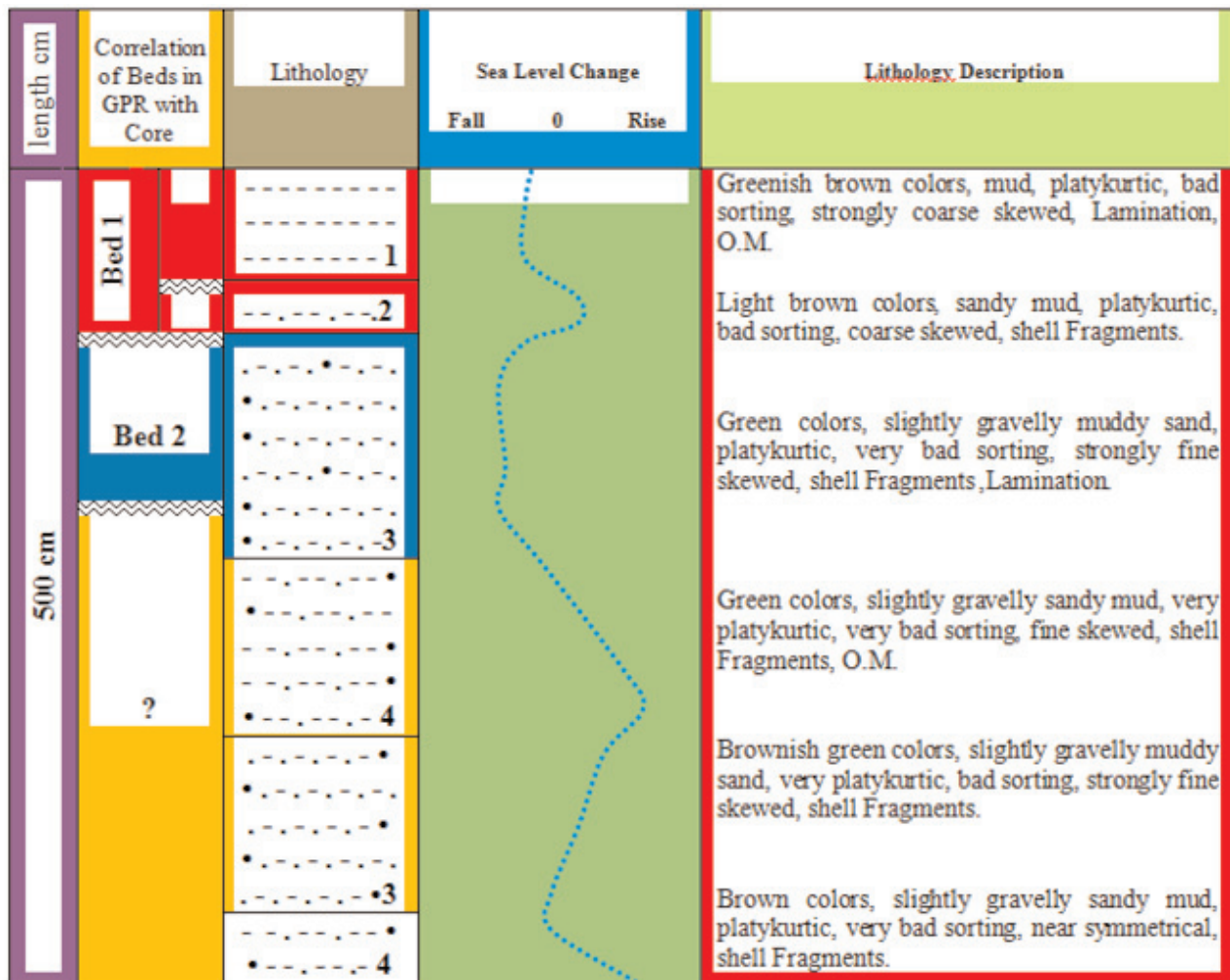


Figure 5. Correlation of layers subsurface in GPR with sediment Core, column facies, relative sea level changes and describes the sediment core L, Parak estuary, scale: 1:100

sedimentary cores, the GPR profiles and their compliance in estuary Shoor and Parak, it was related that the change of sedimentary facies and depositional environment is with changes in particle size.

4-In profiles No.71 and No.72, there are two layers subsurface. Thickness of the first subsurface layer 1 about 4.1m and thickness in the subsurface layer 2 is about 78cm and from the top of point start move towards the sea, the layers thickness increased. The subsurface layer 1 in the profile No.71 and No.72 from the surface to a depth of 90cm with facie 1 in supratidal environment and from depth of 90cm to one meter of depth is identical with facies 2 intertidal environment. So, the subsurface layer 2 in the GPR profiles with the sedimentary units 3 are related to environmental supratidal. Increased thickness of lay-

ers due to expansion of the surface sediments of sand dunes in coast.

5-In profiles No.73 and No.74, there are four layers subsurface. The thickness of subsurface layer 1 about 1.4 m, thickness of subsurface layer 2 about 70cm, thickness of subsurface layer 3 about 40cm and thickness of subsurface layer 4 about has about 84cm. Also, in the GPR profiles, subsurface layer 1 with layers 1 and 2 sediment cores, subsurface layer 2 with layer 3 sediment cores and subsurface layers 3 and 4 are consistent with layer 4 in sediment cores. in the withdrawals from the beginning towards the coastline, the thickness subsurface layer 1 is almost uniform, the thickness subsurface layer 2, first increases and then decreases, the thickness subsurface layer 3, first decreases and then increases again

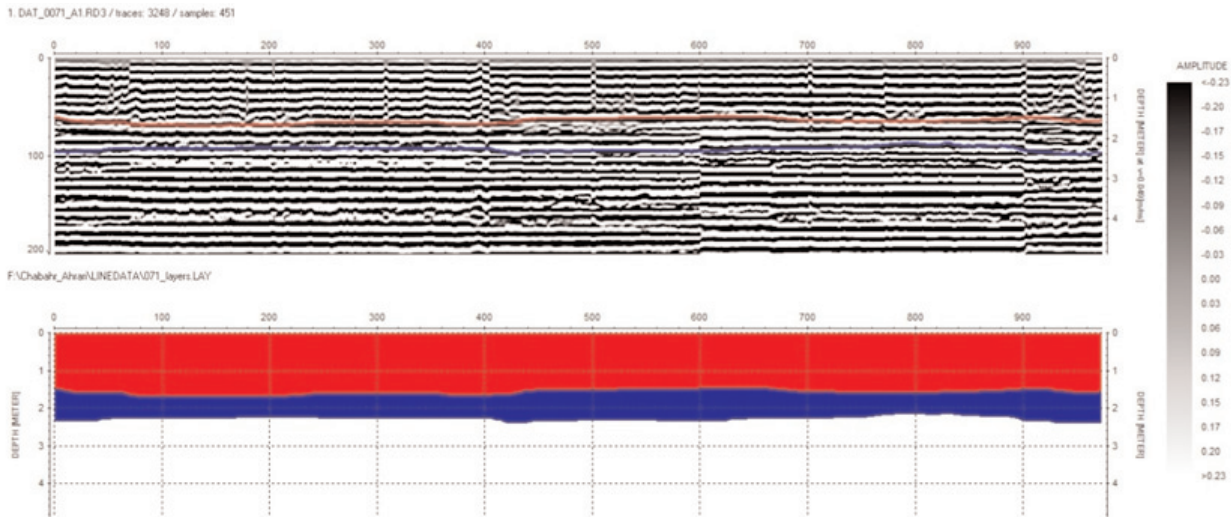


Figure 6. Profile No.71 and its image processing

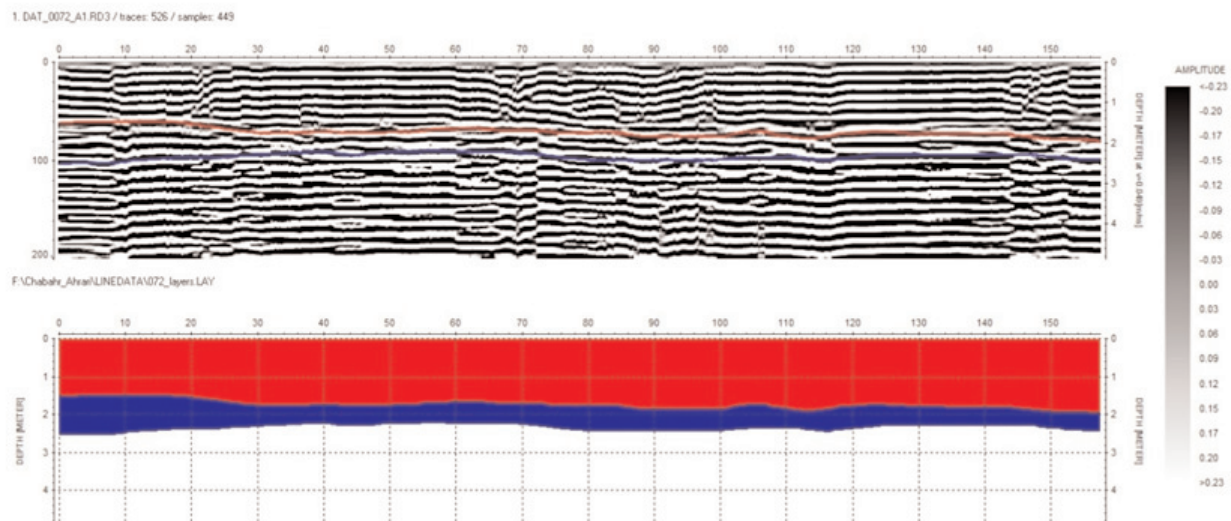


Figure 7. Profiles No.72 and its image processing section

decreases and thickness subsurface layer 4, first increases and then decreases again increases. Thickness changes due to local sea level change that have been deposited tidal sediments.

6-The profile GPR No.73 and No.74 was nearer to the sea and influence the saltwater sea on GPR data. Thus, detection of subsurface structures is less effective and two layers of subsurface has been identified in the Parak estuary, and so in Shoor estuary (the profile GPR No.71 and No.72), high distance from the sea and influence the saltwater sea is less and detection of subsurface structures is stronger that has leading to the identification of four layers of subsurface.

7-These facies which gradually turn related to the

environment Supratidal, intertidal, Supratidal and is intertidal and the two sedimentary cycles include a Raise and lower the water levels locally in the northern Oman Sea are.

8-Comparison of sediment cores and GPR profiles with curve changes in global sea levels show that during two-Interval from time 2100 to 2800 years ago and so from time 4900 to 5800 years ago, increased sedimentation and sedimentation rates higher than average (0.1mm per year) respectively

9-Results of the adaptation of seismic data and sedimentary facies indicate that Changing the particle size, type and depositional environment is related to sediments particle size in the subsurface layers.

10-Depth of effect the penetration wave in GPR profiles of 3.6m is not higher.

11-Differences in sediment type, grain size and amount of clay in the subsurface structures, creates contrast in electrical properties, including differences in the size of the electric permittivity of free space are the main reason for classification theirs in different layers.

12-The morphology of the northern coast of Oman by tectonic processes Plio-Pleistocene formed, although erosion and sedimentation processes has effected of surface modifications. On the other hand, the lower sea level to about 120 - m during the last period of glacial Pleistocene and Maximum (LGM) about 18 to 21 thousand years ago, it was found that exposure to

the northern coast of Oman and they dug channels and rivers in their range, but after the last glacial period, sea level will advance to the basin about 4 to 6 thousand years ago to its maximum approximately 1 to 3m above its current level of receipts.

References

Al- Asfour, T. A., 1978, The marine terraces of the Bay of Kuwait. In: Brice. W. C. (Ed.). The Environmental History of the Near and Middle East Since the Last Ice Age, pp.249-260. Academic Press, Inc: London Ltd.

Benedetto, A. and Pensa, S., 2007, Indirect diagnosis of pavement structural damages using surface GPR reflection techniques, *Journal of Applied Geophysics*, V. 62, No. 2, P. 107-123.

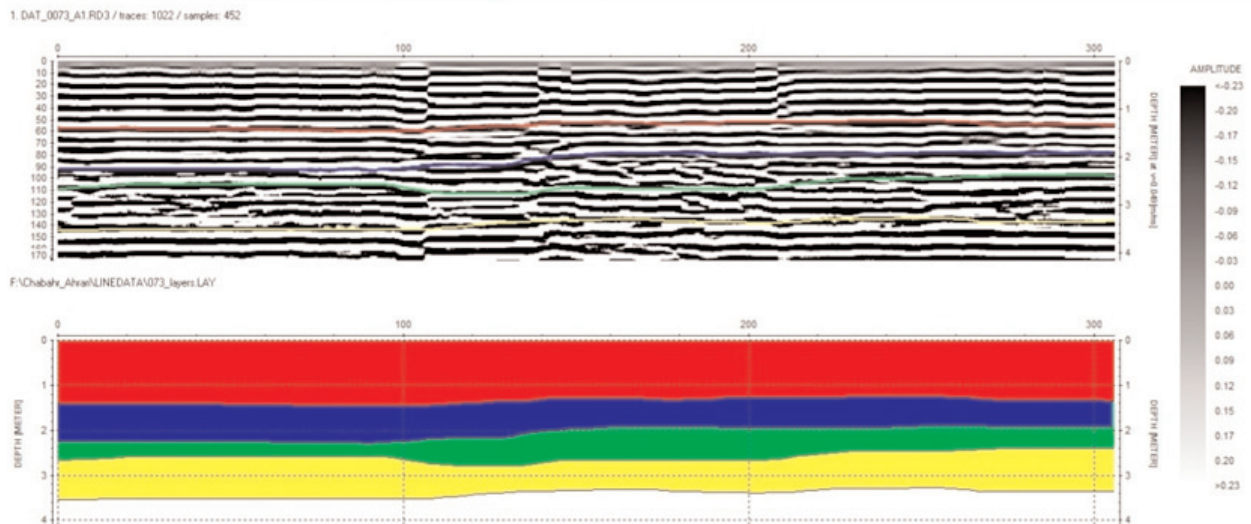


Figure 8. Profiles No.73 and its image processing.

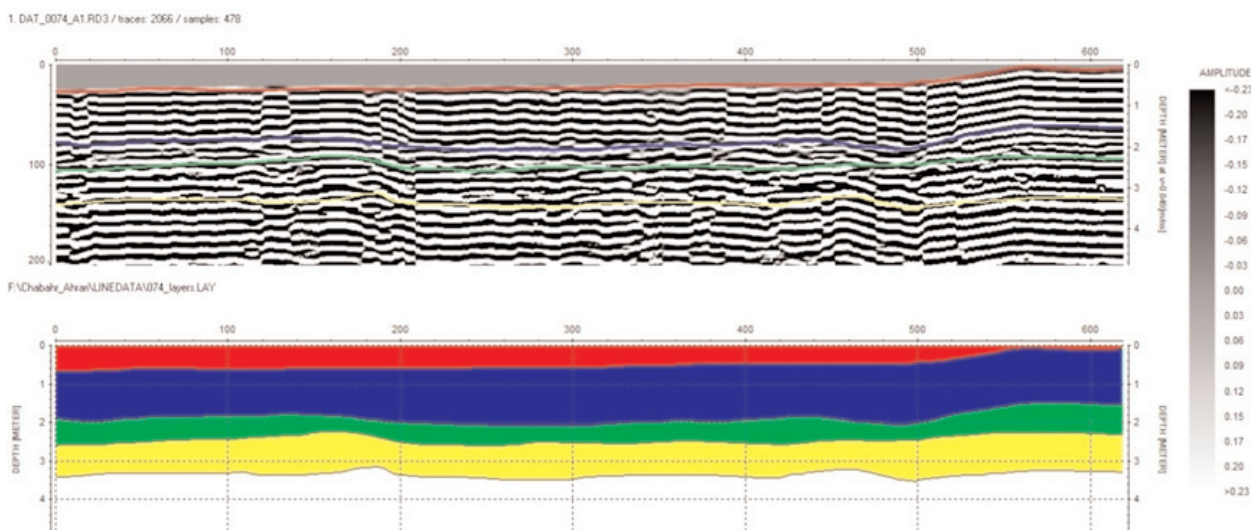


Figure 9. Profiles No.74 and its image processing.

- Bennett, M.R.; Cassidy, N.J. and Pile, J., 2009**, Internal structure of a barrier beach as revealed by ground penetrating radar (GPR): Chesil beach, *Geomorphology*, V. 104, P. 218-229.
- Bird, E., 2008**, Coastal Geomorphology, Second Edition, *University of Melbourne, Australia*, 438 P.
- Bristow, C.S., Jol, H.M., 2003**, Ground penetrating Radar in Sediments, *published by the Geological Society, London*, 339 p.
- Bourrouilh-Le Jan, F.G., 2007**, Very high energy sedimentation (supratidal hurricane deposits) and Mid-Holocene highstand on carbonate platforms, Andros, Bahamas: An alternative view, *Sedimentary Geology*, V. 199, P. 29-49.
- Caldas, L.H.O.; Statterger, K. and Vital, H., 2006**, Holocene sea-level history: Evidence from coastal sediments of the northern Rio Grande do Norte coast, NE Brazil, *Marine Geology*, V. 228, P. 39-53.
- Cameron, W. M. and D.W. Pritchard, 1963**, Estuaries, (M. N. Hill Ed.): The Sea, Wiley, J. and Sons, *New York*, V. 2, P. 306 - 324.
- Carling, P.A.; Radecki-Pawlik, A.; Williams, J.J.; Rumble, B.; Meshkova, L.; Bell, P. and Breakspear, R., 2006**, The morphodynamics and internal structure of intertidal fine-gravel dunes: Hills Flats, Severn Estuary, UK, *Sedimentary Geology*, V. 183, P. 159-179.
- Carpentier, S.F.A.; Green, A.G.; Doetsch, J.A.; Dorn, C.; Kaiser, A.E.; Campbell, F.; Horstmeyer, H. and Finnemore, M., 2011**, Recent deformation of Quaternary sediments as inferred from GPR images and shallow P-wave velocity tomograms: Northwest Canterbury Plains, New Zealand, *Journal of Applied Geophysics*, V. 72, P. 1-14.
- Daniels DJ (ed.), 2004**, Ground Penetrating Radar (2nd Ed.). Knoval (Institution of Engineering and Technology). pp. 1-4. ISBN 978-0-86341-360-5
- Das, B.K.; AL-Mikhlafi, A.S. and Kaur, P., 2006**, Geochemistry of Mansar Lake sediment, Jammu, India: Implication for source-area weathering, provenance, and tectonic setting, *Journal of Asian Earth Sciences*, Elsevier, V. 26, P.649-668.
- Dolati, A., 2010**, Stratigraphy, Structural geology and low-temperature thermochronology across the Makran accretionary wedge in Iran, *Swiss Institute of Technology Zurich, Diss ETH, No. 19151*, 165 P.
- Felber, H., Hotzl, H., Maurin, V., Moser, H., Rauert, W., Zotl, J. G., 1978**, Sea level fluctuations during the Quaternary period. In: Al-Sayyari, S. S., Z?tl, J. G. (Eds.), *Quaternary Period in Saudi Arabia. Springer, New York, Ny*, pp.50-57.
- Folk, R.L., 1974**, Petrology of Sedimentary rocks, Hemphill Publishing Co., *Austin Texas*, 182 P.
- Garcia, D.; Ravenne, C.; Marechal, B. and Moutte, J., (2004)**, Geochemical variability induced by entrainment sorting: quantified signals for provenance analysis, *Sedimentary Geology*, V. 171, P. 113-128.
- Geology of Iran**, Geological Survey of Iran, 2015, www.gsi.ir
- Hofinghoff, J., 2013**, "Resistive Loaded Antenna for Ground Penetrating Radar Inside a Bottom Hole Assembly". *IEEE Transactions on Antennas and Propagation (IEEE) 61 (12)*. doi: 10.1109/TAP.2013.2283604
- Kassler, P., 1973**, Geomorphic evolution of the Persian Gulf. In: B.H. Pursur(Editor), *The Persian Gulf. Holocene Carbonate Sedimentation and Diagenesis in a Shallow Epicontinental Sea. Springer, New York*, pp. 11-32.
- Lambeck, K., 1996**, Shoreline reconstructions for the Persian Gulf since the last glacial maximum. *Earth and Planetary Science Letters 142*, pp. 43- 57.
- Lee, S.H.; Lee, H.J.; Jo, H.R.; Bahk, J.J. and Chu, Y.S., 2005**, Complex sedimentation of the Holocene mud deposits in a ria-type coastal area, eastern Korea Strait, *Marine Geology*, V. 214, P. 389-409.
- Matthew R. Bennett, Nigel J. Cassidy, Jeremy P., 2009**, Internal structure of a barrier beach as revealed by ground penetrating radar (GPR): Chesil beach, UK, *Geomorphology, Volume 104, Issues 3-4, Pages 218-229*
- Miall, A.D., 2000**, Principles of Sedimentary Basin Analysis, Third Edition, *Springer, University of Toronto, Canada*, 616 P.
- 24-Miettinen, A.; Jansson, H.; Alenius, T. and Haggren, G., 2007**, Late Holocene sea-level changes along the southern coast of Finland, Baltic Sea, *Marine Geology*, V. 242, P. 27-38.
- Neal, A. (2003)**, Ground-Penetrating Radar and its use in

- sediment logy: principle, problem and progress: *Earth-science Reviews*, 66, 261-330.
- Railsback, L.B.; Liang, F.; Vidal Romani, J.R.; Grandal-d Anglade, A.; Rodriguez, M.V.; Fidalgo, L.S.; Mosquera, D.F.; Cheng, H. and Edwards, R. L., 2011**, Petrographic and isotopic evidence for Holocene long-term climate change and shorter-term environmental shifts from a stalagmite from the Serra do Courel of northwestern Spain, and implications for climatic history across Europe and the Mediterranean, *Palaeogeography, Palaeoclimatology, Palaeoecology*, V. 305, P. 172-184.
- 27-Rolett, B.V.; Zheng, Z. and Yue, Y., 2011**, Holocene sea-level change and the emergence of Neolithic seafaring in the Fuzhou Basin (Fujian, China), *Quaternary Science Reviews*, V. 30, P. 788-797.
- Tamura, T.; Murakami, F.; Nanayama, F.; Watanabe, K. and Saito, Y., 2008**, Ground-penetrating radar profiles of Holocene raised-beach deposits in the Kujukuri strand plain, Pacific coast of eastern Japan, *Marine Geology*, V. 248, P. 11-27.
- Tucker, M.E., 1988**, Techniques in Sedimentology, In: *Tucker, M.E. (Ed.), Blackwells, Oxford, 394 P.*
- Uchupi, E., Swift, S. A., Ross, D. A., 1996**, Gas venting and late Quaternary sedimentation in the Persian (Arabian) Gulf. *Marine Geology* 129, pp. 237-269.
- Vernant, P.H.; Nilforoushan, F.; Hatzfeld, D.; Abbasi, M.R. Vigny, C.; Masson, F.; Nankali, H.; Matinod, J.; Ashtian, A. and Chery, J., 2004**, Present day crustal deformation and plate kinematics in the Middle East constrained by GPS measurements in Iran and Northern Oman, *Geophysical Journal International*, V. 157 (1), P. 381-398.
- Zhuravlev, A.V.; Ivashov, S.I.; Razevig, V.V.; Vasiliev, I.A.; Türk, A.S.; Kizilay, A., 2013**, "Holographic subsurface imaging radar for applications in civil engineering". (PDF). IET International Radar Conference, Xi'an, China: IET. doi: 10.1049/cp. 2013. 0111.
- Weijermars, R., 1999**, Quaternary evolution of Dawahat Zulum (Half Moon Bay) Region of Eastern Province, Saudi Arabia. *GeoArabia* 4, pp.71-90
- Wilson et al., 2006**, A review of the alluvial diamond industry and the gravels of the North West Province, South Africa (PDF). *South African Journal of Geology* (Geological Society of South Africa) 109 (3): 301-314. doi:10.2113/gssajg.109.3.301. Retrieved 9 December 2012.).
- Woodroffe, S.A. and Horton, B.P., 2005**, Holocene sea-level changes in the Indo-Pacific, *Journal of Asian Earth Sciences*, V. 25, P. 29-43.